

A scheduling and control approach for an industrial furnace to minimise idle energy consumption

Ondřej Benedikt^{a,b}, Baran Alikoç^a, Přemysl Šůcha^a, Sergej Čelikovský^c and Zdeněk Hanzálek^a

^aCzech Institute of Informatics, Robotics and Cybernetics, Czech Technical University in Prague, Czech Republic

^bFaculty of Electrical Engineering, Czech Technical University in Prague, Czech Republic

^cInstitute of Information Theory and Automation, Czech Academy of Sciences, Prague, Czech Republic

ARTICLE HISTORY

Compiled May 18, 2022

ABSTRACT

This article presents a novel scheduling approach to minimise the energy consumption of an industrial furnace during its idle periods. Production tasks characterised by release times and deadlines are scheduled in the given order such that the idle energy consumption of the furnace is minimised. Contrary to the existing approaches, which consider just a finite number of standby modes and time constants to switch between them, our approach provides an efficient combination of both optimal scheduling and optimal control of continuous-time dynamical systems described by ordinary differential equations. Specifically, we consider the temperature control of a single furnace. The furnace dynamics during the idle periods is characterised by the continuous-time bilinear system model, which is analysed using Pontryagin's minimum principle. This way, the scheduling algorithm can exploit the full knowledge of the furnace dynamics encapsulated in the idle energy function. The crucial property shown here is the concavity of the idle energy function, which enables the respective scheduling problem to be solved in polynomial time. Our approach is thoroughly tested using numerical simulations of a real industrial electric furnace model showing that more energy can be saved compared with existing approaches based on the finite number of modes.

KEYWORDS

Scheduling; energy optimisation; operational research; optimal control; electric furnaces.

1. Introduction

The energy consumption optimisation during heat-intensive production processes is the topic of this paper. The practical inspiration comes from Škoda Auto performing steel hardening during the production of automatic gear shafts. The hardening is performed in electric vacuum furnaces, which require a high power input to reach and maintain the specific operating temperature. According to the analysis performed by Škoda Auto in this plant, the highest energy savings can be achieved at this stage.

Despite this inspiration, a successful scheduling solution for the idle energy consumption minimisation problem has clear potential to be applied in many other industrial processes, including the widely spread glass tempering (Módos, Šůcha, and Hanzálek 2017).

As already noted, the operation of various types of furnaces is a highly energy-demanding process, and therefore its energy consumption optimisation usually provides a significant reduction in production costs. Furthermore, energy is often wasted during the prolonged idle periods on maintaining the operating temperature required by the respective technological process. Often, as indeed can be observed in several companies, all furnaces are heated to the operating temperature at the beginning of the week and turned off at the end. This strategy is obviously very wasteful because a considerable amount of energy is consumed for heating even during the idle periods (for more supporting arguments see, e.g. Gutowski et al. 2005; Mouzon, Yildirim, and Twomey 2007; Gahm et al. 2016).

Summarising, efficient scheduling of the idle periods is one of the most important sources of energy savings. The present article provides a new and, to the best of the authors' knowledge, original approach that combines both usual scheduling methods and optimal control of continuous-time dynamical systems described by ordinary differential equations. Our aim is to reduce energy consumption by lowering the temperature of the furnace appropriately during idle periods, while also scheduling the tasks for the previously mentioned heat-intensive production processes.

To do so, a single machine scheduling problem with idle energy consumption minimisation where the order of the tasks is assumed to be fixed is considered here. There are two reasons for assuming this scenario. The first is that idle periods are usually optimised when the production schedule is already fixed. This two-stage view is realistic because production companies frequently see energy consumption as a secondary optimisation objective. Then the optimisation of energy consumption adjusts the start times of tasks within the bounds given by the production schedule. The second reason is that the single machine problem with release times and deadlines is already \mathcal{NP} -hard (Garey and Johnson 1977). Therefore, it is reasonable to solve the entire production problem by a heuristic. In this case, a decision concerning the order of tasks and their assignment to machines is often determined by a local-search or meta-heuristic technique, whereas start times of tasks can be determined by our approach (see Section 4). To study idle energy optimisation, we approximate continuous-time furnace dynamics during the idle period by a bilinear model. It is well-known and accepted approximation for the models involving higher-order nonlinearities. Furthermore, as this model has a one-dimensional state and single input, it enables the complete theoretical analysis using Pontryagin's minimum principle (PMP). This analysis will show, in a mathematically rigorous way, that the optimal strategy during the idle period consists of switching from zero furnace heating to the maximal possible heating at some convenient switching time. This switching time is then shown to result in the concavity of the idle energy function, which enables the respective scheduling problem to be solved in polynomial time. These results are thoroughly tested using numerical simulations of a real industrial electric furnace model showing that more energy can be saved compared with existing approaches, which are limited to model only two (or few) modes of the machine.

1.1. *Related work*

Concerning the research of energy-efficient manufacturing systems, one of the first analyses in this area was performed by Mouzon, Yildirim, and Twomey (2007), who observed that a significant amount of energy could be saved by managing the state of the machine. They proposed several dispatching rules for online production, considering *operating* and *idle* states of the machine. Specifically, rules were devised to turn the non-bottleneck machines off when they were idle for a certain amount of time. Experimental results showed that, compared to the worst-case policy (no switching), substantial energy savings could be achieved. On the other hand, only a single standby mode with constant switching time between modes is assumed by Mouzon et al. However, this assumption might be too restrictive for both the machine dynamics and energy minimisation in reality. Thus, the research of Mouzon et al. was followed by others, who typically simplified the dynamics of the machine by using a transition graph, where vertices correspond to the individual states, and edges represent transitions between them. Edges are typically labelled, as the transition costs and times cannot be neglected. Often, authors consider only a simple case with two states, the *processing* (operational) state and *off* state, which is also the case in the work of Che et al. (2017), who proposed a mixed-integer linear programming (ILP) model and heuristics for bi-objective minimisation of the energy and maximum tardiness. Another example can be found in the work of Liu and Huang (2014), who considered two states (*processing* and *idle*) of a batch-processing machine and employed a genetic algorithm to minimise the total weighted tardiness and carbon footprint. Angel, Bampis, and Chau (2012) analysed a single machine problem with a single standby mode and tasks with release times and agreeable deadlines and showed that the problem of idle energy minimisation can be solved in polynomial time. Machines characterised by three states (*processing*, *idle*, and *shutdown*) were studied by both Shrouf et al. (2014) and Aghelinejad, Ouazene, and Yalaoui (2018), who addressed energy minimisation under variable energy prices.

Regarding heat-intensive production systems and industrial furnaces, the literature is still very sparse. Some authors have studied re-heating furnaces (Zhang et al. 2002; Tang, Ren, and Yang 2014), which are used to heat steel slabs to a specified temperature before they enter the next production stage. Typically, the duration which the slabs spend inside the furnace (i.e. the processing time), and the sequence of the slabs are optimised. Haït and Artigues (2011) studied the problem where the metal is melted in several induction furnaces. The melting time can be shortened by increasing the input power. In contrast, the processing time, as well as the temperature, are specified in our case to ensure the desired quality of the product. Liu et al. (2018) addressed a glass production flow-shop problem, modelling multiple stages, and optimising the makespan and total energy consumption. However, the state of the furnace was modelled only by *processing* and *idle* states.

In addition to the manufacturing processes mentioned previously, the research on power-saving states has a broad base in the domain of embedded systems, where energy savings are crucial to prolonging the battery life (Irani, Shukla, and Gupta 2003; Baptiste, Chrobak, and Dürr 2012; Gerards and Kuper 2013). The considered devices typically have only a small number of power-saving states (Gerards and Kuper 2013), which are specified by the manufacturer. Sometimes authors assume only the *processing state* and the *off-state* (Irani, Shukla, and Gupta 2003; Baptiste, Chrobak, and Dürr 2012). The studied problems commonly lead to online scheduling algorithms because of their real-time character or uncertainties in the arrival times of the tasks.

In contrast to embedded systems, the dynamics of heat-intensive systems are relatively slow. By assuming only on and off states, the idle periods between two consecutive tasks would need to be very long to make the transitions possible. Another difference is the possibility of solving the production problems offline with respect to known, or *a priori* approximated, parameters of the tasks and the identifiable dynamic behaviours. However, despite all differences, some concepts originating from the domain of embedded systems are general and can still be used even for production scheduling. Frequently, the idle energy consumption is captured by an *idle energy function*, $E : \mathbb{R}_{\geq 0} \rightarrow \mathbb{R}_{\geq 0}$, mapping the length of the idle period to energy consumption (Gerards and Kuper 2013). Such a function E is typically assumed to be non-decreasing piecewise-linear concave where each linear segment corresponds to a single power-saving state. We mainly adopt this concept in the scheduling of furnace operations by integrating continuous control that minimises energy consumption during idle periods, instead of considering finite power-saving states. In this sense, we consider the time-domain behaviour of the furnace temperature and its energy-optimal control, then integrating those into the scheduling problem for total idle energy minimisation.

1.2. Contributions and outline

In the context of the existing related works, the main original contributions of the present article are summarised as follows.

- (1) We define the problem of idle energy consumption minimisation for a single machine scheduling with release times, deadlines, and the fixed order of tasks, and show that the problem can be solved in polynomial time with the proposed algorithms, assuming that the idle energy function is concave.
- (2) Utilising a bilinear system approximation of furnace dynamics, we propose an energy-optimal control law for fixed idle period lengths and show that the idle energy function under this control law is concave.
- (3) We show that the obtained idle energy function can be integrated into the proposed scheduling approaches for the idle energy consumption minimisation.
- (4) Identifying a dynamics of a real industrial furnace at Škoda Auto, we verify the proposed approach on a set of instances and show that the proposed solution provides significantly less energy consumption as compared with the existing scheduling approaches.

The rest of the article is organised as follows. Section 2 provides the problem description and assumptions. In Section 3, the dominant structures in schedules are identified, and it is shown that the scheduling problem can be solved in polynomial time. In Section 4, two scheduling approaches optimising the idle energy consumption are described. Section 5 addresses the modelling of the furnace; a bilinear model is described, and energy-optimal control law is derived. The case study in Section 5.3 describes a real furnace used in the production; bilinear model parameters are identified, and the idle energy function is derived. The case study is followed by Section 6, which shows the results of the numerical scheduling experiments using the identified model of the real furnace. Finally, Section 7 concludes the article.

2. Problem statement

We study a single machine scheduling problem to optimise the idle energy consumption where the order of the tasks is assumed to be fixed. For a given fixed order, the start times of the tasks need to be found, such that the total energy consumption during the idle periods is minimised. Energy consumption during the processing of the task is not optimised, because to ensure the quality of the product, the processing time and the operating temperature of the furnace are given and cannot be changed. We assume that the execution of each task is restricted by its release time and deadline. The release time represents the time when the product or part arrives from the previous stage of production, whereas the deadline is given by time demands of the following production/expedition stages. We denote the scheduling problem by $1 | r_j, \tilde{d}_j, \text{fixed order} | \Sigma E$.

2.1. Formal description

Formally, let $T = \{1, 2, \dots, n\}$ denote the set of tasks. Each task $i \in T$ is characterised by three integers: release time $r_i \in \mathbb{Z}_{\geq 0}$, deadline $\tilde{d}_i \in \mathbb{Z}_{> 0}$, and processing time $p_i \in \mathbb{Z}_{> 0}$, such that $r_i + p_i \leq \tilde{d}_i \forall i \in T$.

A schedule is defined by vector of start times $\mathbf{s} = (s_1, s_2, \dots, s_n) \in \mathbb{R}_{\geq 0}^n$. A *feasible schedule* is such a schedule that satisfies the following constraints.

- (C1) Each task i is processed within its execution time window $[r_i, \tilde{d}_i]$.
- (C2) The processing order of the tasks is given and fixed.
- (C3) At most, a single task is processed at one time.
- (C4) The processing is done without preemption.

For the rest of this work, when we talk about a schedule, we always mean a feasible schedule.

The objective is to find start times \mathbf{s} , such that the idle energy consumption $E_{\text{total}}(\mathbf{s})$ (i.e. the total energy consumption during idle periods) is minimised. An *idle period* is defined as the duration between the completion time of a task and start time of the following one. Since the execution order of the tasks is fixed, we can assume that the tasks are sorted in the given order, i.e. $s_i + p_i \leq s_{i+1} \forall i \in \{1, 2, \dots, n-1\}$. Then, the objective can be written as

$$\min_{\mathbf{s}} E_{\text{total}}(\mathbf{s}) = \min_{\mathbf{s}} \sum_{i=1}^{n-1} E(s_{i+1} - (s_i + p_i)), \quad (1)$$

where E represents the *idle energy function*, i.e. the relationship between the idle period length and the consumed energy (taking into account various power-saving modes). The idle energy function, whose shape may have an effect on the problem complexity (see Section 3), is further discussed in Section 5.1.

2.2. Assumptions and constraints considered in the model

We assume that the furnace is turned *on* (heated to the operating temperature from *off* mode) just before the first task is processed, and it is turned *off* (cooled down) immediately after the last task is processed. When the furnace is *off*, the power con-

sumption is zero. Costs for turning the machine on and shutting it off are constant and cannot be optimised.

When a task is processed, the furnace is heated to the operating temperature (same for all tasks) given by the respective technological process. However, during the idle periods, the temperature of the furnace is not specified, and so it can be lowered to save energy. At the end of the idle period, the furnace is heated up again, so that it reaches the operating temperature before the next task is processed.

Note that because of the fixed order, release times and deadlines can be propagated. Specifically, taking tasks from left to right, release times can be shifted such that

$$r_i := \max\{r_{i-1} + p_{i-1}, r_i\}, \quad \forall i \in \{2, 3, \dots, n\}, \quad (2)$$

and taking the tasks from right to left, deadlines can be adjusted such that

$$\tilde{d}_i := \min\{\tilde{d}_{i+1} - p_{i+1}, \tilde{d}_i\}, \quad \forall i \in \{n-1, n-2, \dots, 1\}. \quad (3)$$

If there exists a task such that its propagated execution window is shorter than its processing time, then the instance does not have a feasible solution for the given order. For the rest of this article, we assume that release times and deadlines are propagated and a feasible solution exists.

3. Complexity analysis

In this section, we show that $1|r_j, \tilde{d}_j, \text{fixed order}|\Sigma E$ can be solved in polynomial time under the assumption that the energy function E is concave. Note that if the order was not fixed, the problem would be \mathcal{NP} -hard because its underlying problem $1|r_j, \tilde{d}_j|-$ is \mathcal{NP} -complete in a strong sense (Garey and Johnson 1977).

A special version of the problem studied here was addressed by Gerards and Kuper (2013), who assumed a so-called *frame-based system*, i.e. a system where $r_i = (i-1) \cdot T$ and $\tilde{d}_i = i \cdot T$. In frame-based systems, execution windows of the tasks do not overlap. Gerards and Kuper showed that idle energy minimisation in frame-based systems can be done in polynomial time, assuming that the idle energy function is concave. We extend their result to $1|r_j, \tilde{d}_j, \text{fixed order}|\Sigma E$, i.e. to systems with arbitrary release times and deadlines, assuming that the execution order of the tasks is fixed.

3.1. Definitions

Before providing the complexity analysis, let us describe a structure that appears in the feasible schedules. It is called a *block of tasks* or simply *block*, and is widely used; see, e.g. Baker and Trietsch (2009) or Baptiste, Chrobak, and Dürr (2012).

Definition 3.1 (Block of tasks). A sequence of tasks $B = (b_1, \dots, b_m)$, which are scheduled on the same machine, is called a block of tasks if the following properties hold:

$$s_{b_i} + p_{b_i} = s_{b_{i+1}}, \quad \forall i \in \{1, 2, \dots, m-1\}, \quad (4)$$

$$\forall i \in T \setminus B : (s_i + p_i < s_{b_1}) \vee (s_i > s_{b_m} + p_{b_m}). \quad (5)$$

Every feasible schedule is composed of blocks of tasks, which are separated by

idle intervals. Blocks are, therefore, fundamental building elements out of which the resulting schedule is created. Property (5) states that block B is maximal, i.e. it cannot be extended to the left or right.

Even though all schedules are composed of blocks of tasks, some schedules are special in a certain sense. We call them *block-form schedules*.

Definition 3.2 (Block-form schedule). A schedule consisting of k blocks B_1, B_2, \dots, B_k is in the *block form* if each block of tasks B_j contains at least one task, which starts at its (propagated) release time or ends at its (propagated) deadline; such a task is called a *support* of block B_j .

Thanks to the properties of the block-form schedules, the idle energy optimisation can be made simple, as shown in Section 3.2 and Section 3.3.

3.2. Dominance of block-form schedules

In this section, we show that block-form schedules weakly dominate all other schedules. To prove this, we utilise the following lemma.

Lemma 3.3. *Given a concave idle energy function $E : \mathbb{R}_{\geq 0} \rightarrow \mathbb{R}_{\geq 0}$, for $0 \leq \epsilon \leq x \leq y$ it holds that*

$$E(x - \epsilon) + E(y + \epsilon) \leq E(x) + E(y). \quad (6)$$

Proof. Property (6) is directly implied by the concavity of E , see Gerards and Kuper (2013). \square

Lemma 3.3 implies that, in the case of having two idle periods x and y , energy $E(x) + E(y)$ decreases or remains the same even if the shorter idle period of length x is reduced on behalf of the longer idle period of length y . Then, we have the following theorem.

Theorem 3.4. *Given a concave idle energy function E , for every feasible schedule S_1 defined by start times \mathbf{s}_1 , there exists a feasible schedule S_2 defined by start times \mathbf{s}_2 , such that S_2 is in a block form and $E_{total}(\mathbf{s}_1) \geq E_{total}(\mathbf{s}_2)$.*

Proof. If S_1 is already in a block form, nothing has to be done. Otherwise, S_1 consists of k blocks

$$\{B_1, B_2, \dots, B_k\} = \mathcal{B}_{\text{fixed}} \cup \mathcal{B}_{\text{free}}, \quad \mathcal{B}_{\text{fixed}} \cap \mathcal{B}_{\text{free}} = \emptyset,$$

where $\mathcal{B}_{\text{fixed}}$ is the set of blocks that contain at least one support, and $\mathcal{B}_{\text{free}}$ are the blocks without supports. The blocks in $\mathcal{B}_{\text{fixed}}$ will not be moved, while the blocks in $\mathcal{B}_{\text{free}}$ will be shifted to gain a support. By *shift*, we mean adding a non-zero constant to all start times of the tasks in the block.

Let us assume that there is an infinitely long idle period before the first block in S_1 and after the last one. Now, every block is separated from the other blocks by two idle periods (before and after the block).

Let us take an arbitrary block $B \in \mathcal{B}_{\text{free}}$. Since it does not contain a support, it can be shifted. The direction of the shift can be selected according to Lemma 3.3 such that the idle energy consumption does not increase (i.e. shift the block such that the shorter

neighbouring idle period decreases its length). Note that the leftmost (rightmost) block is always shifted right (left) to prolong the time when the machine is off (idle energy consumption does not increase).

After the block is shifted as much as possible, there are two possible outcomes.

- (1) Some task $i \in B$ reaches its release time or deadline.
 In this case, block B gains a support and joins $\mathcal{B}_{\text{fixed}}$; the cardinality of $\mathcal{B}_{\text{free}}$ decreases by one.
- (2) Block B reaches its neighbouring block B_{neigh} .
 In this case, block B joins its neighbouring block. If $B_{\text{neigh}} \in \mathcal{B}_{\text{fixed}}$, then B gains a support and joins $\mathcal{B}_{\text{fixed}}$. Otherwise, $\mathcal{B}_{\text{free}} := (\mathcal{B}_{\text{free}} \setminus \{B, B_{\text{neigh}}\}) \cup \{B \oplus B_{\text{neigh}}\}$, i.e. B and B_{neigh} are joined (operator \oplus). Anyway, the cardinality of $\mathcal{B}_{\text{free}}$ decreases by one.

If cases 1. and 2. happen at the same time, both B and B_{neigh} gain a support, join $\mathcal{B}_{\text{fixed}}$, and the cardinality of $\mathcal{B}_{\text{free}}$ decreases by at least one.

It can be seen that after one shift, the cardinality of $\mathcal{B}_{\text{free}}$ decreases, and the idle energy consumption does not increase (by Lemma 3.3). By iteratively shifting the blocks without supports, every block will eventually join $\mathcal{B}_{\text{fixed}}$. Since there are at most n blocks in $\mathcal{B}_{\text{free}}$ at the beginning, and the cardinality of $\mathcal{B}_{\text{free}}$ decreases after each shift, $\mathcal{B}_{\text{free}}$ will be empty after at most n iterations. Also, there are at most n tasks in each block. Therefore, each shift can be done in $\mathcal{O}(n)$ steps (shifting one task after another). Hence, the transformation can be done in $\mathcal{O}(n^2)$ steps. Schedule S_2 is then given by the start times of the tasks in $\mathcal{B}_{\text{fixed}}$. \square

Theorem 3.4 shows that it is sufficient to optimise only over schedules in the block form.

3.3. Finding an energy-optimal block-form schedule

Here we show how the schedules can be represented as paths in an oriented directed acyclic *energy graph*. The graph-based approach was originally introduced for frame-based systems by Gerards and Kuper (2013), but since the release times and deadlines in their frame-based systems do not overlap, the graph had a very simple structure. In our case, we need to non-trivially extend the idea, relying on Theorem 3.4.

By Definition 3.2, each block of a block-form schedule contains at least one support. The main idea leading to a graph-based approach is to represent the supports of the schedule by nodes of the energy graph. In the following, we will show that paths in the energy graph can be associated with the block-form schedules, and the shortest path corresponds to the optimal block-form schedule.

Our extended version of the energy graph can be represented as a triplet $G = (V_G, E_G, c)$, where V_G is set of its vertices, E_G is set of its oriented edges, and $c : E_G \rightarrow \mathbb{R}_{\geq 0}$ is the cost function. For each task $i \in T$, we define vertices v_i^r and $v_i^{\tilde{d}}$ representing situations when task i starts at its release time and ends at its deadline, respectively. Let $\text{start}(v_i^x)$ be the actual start time of the task i represented by vertex v_i^x , i.e.

$$\text{start}(v_i^x) = \begin{cases} r_i, & \text{if } x \text{ is } r, \\ \tilde{d}_i - p_i, & \text{if } x \text{ is } \tilde{d}. \end{cases} \quad (7)$$

Furthermore, let us define two additional dummy vertices, the starting vertex v^s and the ending vertex v^e . We will define the edges in such a way that the paths between v^s and v^e represent block-form schedules. The set of edges E_G consists of three types of edges, $E_G = E_G^{(1)} \cup E_G^{(2)} \cup E_G^{(3)}$, where

$$E_G^{(1)} = \left\{ (v^s, v_i^x) \mid i \in T, x \in \{r, \tilde{d}\} \text{ such that the partial schedule given by } \right. \\ \left. s_i := \text{start}(v_i^x), s_{i'} := s_i - \sum_{k=i'}^{i-1} p_k \forall i' \in \{1, 2, \dots, i-1\} \text{ is feasible} \right\}, \quad (8)$$

$$E_G^{(2)} = \left\{ (v_i^x, v^e) \mid i \in T, x \in \{r, \tilde{d}\} \text{ such that the partial schedule given by } \right. \\ \left. s_i := \text{start}(v_i^x), s_{i'} := s_i + \sum_{k=i}^{i'-1} p_k \forall i' \in \{i+1, i+2, \dots, n\} \text{ is feasible} \right\}, \quad (9)$$

$$E_G^{(3)} = \left\{ (v_i^x, v_{i'}^y) \mid i \in T, i' \in T, i < i', x, y \in \{r, \tilde{d}\} \text{ and } \right. \\ \left. \exists k \in \{i, i+1, \dots, i'-1\} \text{ such that the partial schedule given by } \right. \\ \left. s_i := \text{start}(v_i^x), s_{i'} := \text{start}(v_{i'}^y), \right. \\ \left. s_a := s_i + \sum_{l=i}^{a-1} p_l \forall a \in \{i+1, i+2, \dots, k\}, \right. \\ \left. s_b := s_{i'} - \sum_{l=b}^{i'-1} p_l \forall b \in \{k+1, \dots, i'-1\} \text{ is feasible} \right\}. \quad (10)$$

In $E_G^{(1)}$, edges connect the starting vertex v^s and vertex v_i^x , $x \in r, \tilde{d}$, $i \in T$, associated with task i . Each edge represents the situation when task i is the support and tasks $\{1, 2, \dots, i-1\}$ are aligned to the right, joining the block supported by task i . Similarly, edges in $E_G^{(2)}$ link v_i^x , $x \in r, \tilde{d}$, $i \in T$, with the ending vertex v^e . Each edge represents the situations when task i is the support, and tasks $\{i+1, i+2, \dots, n\}$ are aligned to the left, joining the block supported by i . Finally, set $E_G^{(3)}$ represents situations when there are two blocks of tasks supported by i and i' , respectively. All the tasks $\{i+1, i+2, \dots, k\}$ are aligned to the left and join the block supported by i and tasks $\{k+1, k+2, \dots, i'-1\}$ are aligned to the right and join the block supported by task i' .

Now, we define the cost function c . We set the costs of edges in $E_G^{(1)}$ and $E_G^{(2)}$ to zero because the tasks represented by these edges are processed without any idle periods. The costs of edges in $E_G^{(3)}$ correspond to the idle energy consumption between two blocks of tasks. Even though there might be multiple possible ways to schedule the tasks between the two supports, the processing time of each task is assumed to be constant and so the length of the idle period is invariant for a fixed pair of supports. Let us denote the length of the idle period between blocks supported by v_i^x and $v_{i'}^y$, where $i' > i$, by $t_f(v_i^x, v_{i'}^y)$, defined by

$$t_f(v_i^x, v_{i'}^y) = \text{start}(v_{i'}^y) - (\text{start}(v_i^x) + p_i) - \sum_{k=i+1}^{i'-1} p_k. \quad (11)$$

Now, the cost function can be defined in the following way:

$$c(e) = \begin{cases} 0, & \text{if } e \in E_G^{(1)} \cup E_G^{(2)}, \\ E(t_f(v_i^x, v_{i'}^y)), & \text{if } e = (v_i^x, v_{i'}^y) \in E_G^{(3)}. \end{cases} \quad (12)$$

Explanatory example. To illustrate the energy graph, let us consider an arbitrary concave idle energy function E and four tasks characterised by parameters given in Table 1. The corresponding energy graph is shown in Figure 1. Each edge e is labelled by its cost $c(e)$, defined by (12).

Note that there is no edge between v^s and v_3^r because if task 3 started at its release time, it would not be possible to execute the previous tasks without introducing an idle period ($\tilde{d}_2 = 40 < 45 = r_3$). But in that case, the previous tasks would form a different block, having its own support. Therefore, edge (v^s, v_3^r) does not bring any additional useful information. The situation is similar for other ‘missing’ edges.

Table 1. Example task parameters.

i	1	2	3	4
r_i	0	15	45	80
\tilde{d}_i	20	40	70	100
p_i	10	15	5	10

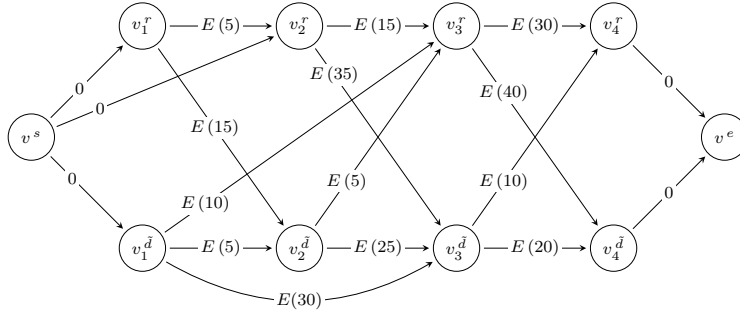


Figure 1. Energy graph constructed for the tasks specified by Table 1.

Having defined vertices, edges, and the cost function, we now see the whole structure of the energy graph. Note that the graph can be constructed in polynomial time. Indeed, it is directed, acyclic, and does not contain parallel edges. There are $\mathcal{O}(n)$ vertices and at most $\mathcal{O}(n^2)$ edges. Whether edge e belongs to the graph or not can be verified according to (8)–(10) in linear time $\mathcal{O}(n)$. Therefore, the number of steps needed to build the graph is upper bounded by $\mathcal{O}(n^3)$.

The connection between the paths in the energy graph and block-form schedules is explained by the following two lemmas.

Lemma 3.5. *For every block-form schedule S , there exists a path in the corresponding energy graph, such that length of the path equals the idle energy consumption of schedule S .*

Proof. This is assured by the structure of the energy graph. Given a block-form schedule with blocks B_1, B_2, \dots, B_k and their supports a_1, a_2, \dots, a_k , the correspond-

ing path in the energy graph is $v^s, v_{a_1}^{x(a_1)}, v_{a_2}^{x(a_2)}, \dots, v_{a_k}^{x(a_k)}, v^e$, where

$$x(a_i) := \begin{cases} r & \text{if } a_i \text{ starts at its release time,} \\ \tilde{d} & \text{if } a_i \text{ ends at its deadline.} \end{cases} \quad (13)$$

Nodes on the path correspond to the supports of the individual blocks, and because the cost of each edge directly corresponds to the idle energy consumption, the length of the path is the same as the idle energy consumption of the schedule. \square

Lemma 3.6. *For every path P between the start node v^s and end node v^e in the energy graph, there exists a feasible block-form schedule S , such that the idle energy consumption cost of S is the same as the length of path P .*

Proof. Again, this is trivially given by the structure of the energy graph, where nodes represent supports of the blocks. According to (8)–(10), an edge between two supports is added only if there exists a feasible schedule of the tasks between them. \square

Remark 1. Note that edges in $E_G^{(3)}$ might not imply one particular schedule of the tasks between the supports. Therefore, for a given path, there might exist multiple feasible schedules with the same idle energy consumption. Similarly, as each block might contain multiple supports, there might be multiple different paths corresponding to one block-form schedule.

Finally, by Lemmas 3.5 and 3.6, we see that problem $1 \mid r_j, \tilde{d}_j, \text{ fixed order} \mid \Sigma E$ can be solved by finding the shortest path in a directed acyclic graph. That can be done in linear time with respect to the size of the graph (Cormen et al. 2001, sec. 24.2). The graph contains $\mathcal{O}(n^2)$ edges and so the overall time needed to find the shortest path is bounded by $\mathcal{O}(n^2)$. The graph itself is constructed in $\mathcal{O}(n^3)$, and so the overall complexity is also $\mathcal{O}(n^3)$.

Explanatory example (continued). The schedule corresponding to path $v^s, v_1^{\tilde{d}}, v_3^r, v_4^r, v^e$ is depicted in Figure 2. It consists of three blocks, $B_1 = (1, 2)$, $B_2 = (3)$, and $B_3 = (4)$. Supports of these blocks are tasks 1, 3 and 4, respectively. Idle energy consumption of the schedule equals the sum of energy consumed during the first idle period (from time 35 to time 45), plus energy consumed during the second idle period (from time 50 to time 80).

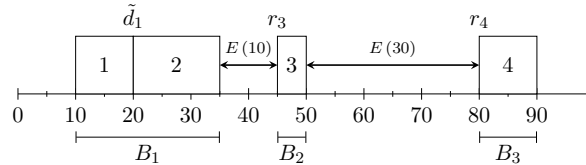


Figure 2. Feasible schedule corresponding to path $v^s, v_1^{\tilde{d}}, v_3^r, v_4^r, v^e$.

Remark 2. The graph-based approach described above can handle arbitrary concave idle energy function, which is a common shape of the idle energy function used in the literature (Irani, Shukla, and Gupta 2003; Gerards and Kuper 2013). However, it is still an open question if the problem would be polynomial even if the idle energy function were not concave (such as function E_{600} shown in Section 5.3.2).

Remark 3. The energy graph could also be used to find the schedules minimising the number of idle periods longer than 0. Such an application is useful when the stress of the machine caused by excessive switching needs to be minimised. The problem reduces again to the shortest path problem. The structure of the graph remains the same, but the edges in $E_G^{(3)}$ should be labelled by some positive constant, e.g. 1. Note that it is again possible to optimise only over the block-form schedules because the shifts described in the proof of Theorem 3.4 might join some blocks but never split them.

4. Scheduling approaches to $1 | r_j, \tilde{d}_j, \text{fixed order} | \Sigma E$

In this section, we describe scheduling approaches that can be used to find start times of the tasks. The first relies on the construction of the energy graph as described in the previous section, while the second uses a mathematical program to model the problem.

4.1. Approach 1: Energy graph

The optimal schedule can be found by solving the shortest path problem, as described in Section 3.3. At first, the directed acyclic energy graph containing $\mathcal{O}(n^2)$ edges is built in $\mathcal{O}(n^3)$ steps. Afterwards, the shortest path is found in linear time with respect to the size of the graph. The advantage of this approach is that the optimal schedule can be found in polynomial time.

4.2. Approach 2: Mathematical program

Another option is to formulate the problem as a mathematical program and call a specialised solver to find the solution. This option is considered, because: (i) mathematical models are easy to modify when additional constraints or different objectives need to be considered, and (ii) the optimisation works even if the function is not concave.

Here, we consider a mixed-integer linear programming approach to model the problem. The disadvantage is that the polynomial running time is not guaranteed. Also, the standard solvers, such as Gurobi or CPLEX, cannot optimise arbitrary functions. Therefore, the non-linear energy function E needs to be approximated by a piecewise linear function. This approximation might lead to suboptimal solutions when the number of segments is low, or to slower running time when the number of segments is high.

The structure of the mathematical program is very simple. The only variables are the continuous variables representing start times, $s_i \in \mathbb{R}_{\geq 0} \forall i \in T$. The whole model is described as

$$\min_{\mathbf{s}} \sum_{i=2}^n E_{\text{pwl}}(s_i - (s_{i-1} + p_{i-1})) \quad (14)$$

$$\text{s.t. } r_i \leq s_i \leq \tilde{d}_i - p_i, \forall i \in T, \quad (15)$$

$$s_i + p_i \leq s_{i+1}, \forall i \in \{1, 2, \dots, n-1\}. \quad (16)$$

The function E_{pwl} is the piecewise-linear approximation of idle energy function E . Constraints (15) specify the execution windows of tasks, whereas constraints (16)

enforce the order of the tasks and forbid the overlaps.

5. Furnace modelling, optimal control, and idle energy function

In this section, we discuss the furnace models and present a bilinear modelling approach, which is shown to provide a good approximation of industrial electric furnaces. Further, the open-loop control for minimum energy consumption during idle periods, concerning the studied scheduling problem, is given based on the considered bilinear system approximation. Then, we show that the idle energy function as an input to the scheduling problem is concave under the proposed approximation and control, allowing the proposed graph-based algorithm to be performed. Finally, the proposed approach is shown on a real industrial electric vacuum furnace from Škoda Auto in Section 5.3.

5.1. A bilinear model approximation of furnaces

Obtaining a reasonable physical model of an industrial furnace is usually very difficult. Some of the problems associated with the furnace modelling are: (i) thermal resistivity of insulators, typically modelled as constant, is temperature-dependent and difficult to identify; (ii) properties of the material may not be homogeneous owing to material imperfections and may change in time because of material degradation; (iii) some physical parameters are unknown or hard to obtain (Chee Chook and Tan 2007). Thus, instead of proposing a physical model and identifying its parameters, it is usual in practice to approximate the furnace dynamics with reasonable linear and nonlinear mathematical models; see, e.g. Wang and Spanos (2002) for a linear model, Moon and Lee (2003) for a fuzzy system approximation, Wang, Hang, and Zou (1998) for a direction-dependent model, and Yu (2000); Chee Chook and Tan (2007) for bilinear system approximations.

Our decision to use the bilinear approximation of the furnace dynamics is motivated by the existing literature. Indeed, Derese and Nodulus (1980) have reported that the bilinear model for heat-transfer processes is more suitable than the linear model. Chee Chook and Tan (2007) considered the identification of a first-order bilinear model for an electric tube furnace and showed experimentally that the bilinear model provides the most accurate description as compared with the linear and direction-dependent models. Another advantage of the bilinear model is its simplicity and well-understood behaviour in the class of nonlinear systems. Thus, we also consider the approximation of the furnace dynamics similarly as in Chee Chook and Tan (2007) with the bilinear model

$$\dot{x}(t) = -\alpha x(t) + \beta u(t) - \rho x(t)u(t), \quad x(t) \in \mathbb{R}, \quad u(t) \in [0, \bar{u}], \quad \alpha, \beta, \rho \in \mathbb{R}_{>0} \quad (17)$$

where u is the applied electric power (in kilowatts), i.e. the input to the system, and x is the deviation of the furnace temperature T_f from the ambient temperature T_e , $x(t) := T_f(t) - T_e$, i.e. the variable to be controlled. The model (17) slightly differs from that in Chee Chook and Tan (2007), because we additionally accommodate constraints on control and system parameters regarding the reality for furnaces. First, we do impose the upper bound \bar{u} on the admissible control power, which is important in practice. Second, based on physical modelling considerations, it is assumed in (17) that the system parameters α , β , and ρ are positive constants. A simplified physical

model of electric furnaces is also given in Chee Chook and Tan (2007) by

$$\dot{T}_f(t) = \frac{1}{C_f} \left(-\frac{T_f(t) - T_e}{R} + u(t) - K(T_f^4(t) - T_e^4) \right) \quad (18)$$

where C_f is the thermal capacitance, R is the thermal resistance, and K is a constant regarding the emissivity of the furnace. Indeed, C_f , R , and K are all positive quantities. Note that T_e is assumed constant both in (17) and (18). Then, it is easy to see that α and β can be, indeed, assumed as positive constants owing to the form of the linear terms both in (17) and (18). In addition, the nonlinear term in (18) is approximated by the bilinear term in (17); moreover, both these terms take positive values in time, which suggests also considering ρ as a positive constant. Note that these constraints hold for the identified parameters of an electrical tube furnace in Chee Chook and Tan (2007) and will also hold for the electrical vacuum furnace, which is studied in Section 5.3 as a case study. Indeed, as shown in Section 5.3.1 later on, these parameters α , β , ρ can be quite precisely identified based on real furnaces data, and the resulting estimates comply with the above assumptions.

5.2. Minimum-energy control and the related idle energy function

This subsection aims to study the optimal control of furnaces during an idle period, based on the approximate bilinear model (17).

It is a common approach during industrial process control to drive the plant using the open-loop (feedforward) control to the operating (or reference) point applying an admissible input and then to switch to closed-loop (feedback) control with an appropriate controller when the operating point (or a threshold value close to the operating point) is reached. This control strategy can be seen in our case study in Section 5.3 from the temperature data of the real industrial furnace controlled to operate at different temperatures (see Figure 3).

Recall that our aim is to find an energy-efficient behaviour of the furnace in an idle period. Thus, we look for an optimal control law, which minimises the power consumption for any fixed idle period length. Then, our problem for furnaces turns into finding a control minimising the performance index

$$J(u) = \int_0^{t_f} |u(t)| dt \quad (19)$$

which is called as minimum-control-effort problem (Kirk 2004). Obviously, t_f can be considered as the idle period length, then $J(u)$ is the energy (in kilowatt-hours) consumed during the idle period. Note, that it is sufficient to consider an open-loop control to heat the furnace to the (close neighbourhood of) operating temperature at the end of the idle period (assuming constant ambient temperature), whereas a closed-loop control is necessary to maintain the operating temperature. As we seek a control minimising energy consumption during the idle periods, we give the following theorem for the open-loop optimal control problem for the industrial furnaces which can be modelled as the bilinear system in (17).

Theorem 5.1. *Consider the following optimal control problem: minimise the perfor-*

mance index (19) subject to constraints

$$x(0) = x(t_f) = x_0 \in \mathbb{R}, \quad x_0 > 0, \quad (20)$$

where $x(t)$ is the solution of the system (17) and $t_f > 0$ is a given fixed terminal time. Further, assume that

$$(\beta - \rho x_0)\bar{u} - \alpha x_0 > 0, \quad (21)$$

where \bar{u} is the upper bound on $u(t)$. Then there exists the unique optimal control $u^*(t)$ solving the above-defined optimal control problem and this optimal control takes the following form

$$u^*(t) = \begin{cases} 0, & \forall t \in [0, t_{sw}) \\ \bar{u}, & \forall t \in [t_{sw}, t_f], \end{cases} \quad (22)$$

where $t_{sw} \in (0, t_f)$ is the switching time. Finally, t_{sw} is the solution of the following equation

$$x_0 = \exp((-\alpha - \rho\bar{u})(t_f - t_{sw})) \left(x_0 \exp(-\alpha t_{sw}) - \frac{\beta\bar{u}}{\alpha + \rho\bar{u}} \right) + \frac{\beta\bar{u}}{\alpha + \rho\bar{u}}, \quad (23)$$

this solution exists and is unique for any given $t_f > 0$.

Proof. Pontryagin's minimum principle (PMP) is used (Kirk 2004). To do so, realise that $|u(t)|$ in (19) can be replaced simply by $u(t)$ because $u(t) > 0 \forall t$ in (17). Further, the appropriate Hamiltonian function for the performance index (19) and the system (17) is given by

$$H(x(t), u(t), \psi(t)) = u(t) - \alpha\psi(t)x(t) + \psi(t)[\beta - \rho x(t)]u(t) \quad (24)$$

where $\psi(t)$ represents the usual adjoint variable. By PMP, the necessary conditions for $u^*(t)$ to be an optimal control are

$$\dot{x}^*(t) = \frac{\partial H(x^*, u^*, \psi^*)}{\partial \psi} = -\alpha x^*(t) + \beta u^*(t) - \rho x^*(t)u^*(t), \quad (25a)$$

$$\dot{\psi}^*(t) = -\frac{\partial H(x^*, u^*, \psi^*)}{\partial x} = \psi^*(t)(\rho u^*(t) + \alpha), \quad \psi(0) = \psi_0 \in \mathbb{R} \setminus \{0\}, \quad (25b)$$

$$H(x^*(t), u^*(t), \psi^*(t)) = \min_{u \in [0, \bar{u}]} H(x^*(t), u(t), \psi^*(t)) \quad \forall t \in [0, t_f] \Rightarrow \quad (25c)$$

$$u^*(t) + \psi^*(t)[\beta - \rho x^*(t)]u^*(t) = \min_{u \in [0, \bar{u}]} (u(t) + \psi^*(t)[\beta - \rho x^*(t)]u(t)) \quad \forall t \in [0, t_f]. \quad (25d)$$

Indeed, the boundary conditions (20) of the investigated control problem are fixed, so that $\psi(t)$ can be any nontrivial solution of the adjoint equation (25b).

Before analysing the above necessary condition for the optimality, let us give the following property useful later on. Namely, (25a) and (25b) can be solved analytically giving that

$$x^*(t) = \exp\left(-\alpha t - \rho \int_0^t u^*(\eta) d\eta\right) \left(x_0 + \beta \int_0^t \exp\left(\int_0^\eta (\alpha\eta + \rho u^*(s)) ds\right) u^*(\eta) d\eta\right), \quad (26)$$

$$\psi^*(t) = \psi_0 \exp\left(\alpha t + \rho \int_0^t u^*(\eta) d\eta\right). \quad (27)$$

To analyse (25a)–(25d) subject to the control constraint $u(t) \in [0, \bar{u}]$, consider the function

$$\phi(\psi^*(t), x^*(t)) = \psi^*(t)(\beta - \rho x^*(t)) + 1 \quad (28)$$

to investigate the minimum of the Hamiltonian with respect to u . Further, realise that the necessary condition (25c)–(25d) implies that $u(t) = \bar{u}$ if $\phi(\psi^*(t), x^*(t)) < 0$; $u(t) = 0$ if $\phi(\psi^*(t), x^*(t)) > 0$; whereas for $\phi(\psi^*(t), x^*(t)) = 0$ it is always satisfied. As a consequence, the optimal control, if it exists, satisfies

$$u^*(t) \begin{cases} = \bar{u}, & \text{for } \phi(\psi^*(t), x^*(t)) < 0 \\ = 0, & \text{for } \phi(\psi^*(t), x^*(t)) > 0 \\ \in [0, \bar{u}], & \text{for } \phi(\psi^*(t), x^*(t)) = 0. \end{cases} \quad (29)$$

Furthermore, by (26) and (27) it holds that

$$\begin{aligned} \phi(t) &= 1 - \psi_0 x_0 \rho + \psi_0 \beta \exp\left(\alpha t + \rho \int_0^t u(\eta) d\eta\right) \\ &\quad - \psi_0 \beta \rho \int_0^t \exp\left(\alpha t + \rho \int_0^\eta u(s) ds\right) u(\eta) d\eta, \\ \frac{d\phi(t)}{dt} &= \psi_0 \beta (\alpha + \rho u(t)) \exp\left(\alpha t + \rho \int_0^t u(\eta) d\eta\right) \\ &\quad - \psi_0 \beta \rho u(t) \exp\left(\alpha t + \rho \int_0^t u(\eta) d\eta\right), \end{aligned} \quad (30)$$

which implies

$$\frac{d\phi(t)}{dt} = \psi_0 \alpha \beta \exp\left(\alpha t + \rho \int_0^t u(\eta) d\eta\right). \quad (31)$$

Now, using (30) and (31) one concludes that

$$\phi(0) = \psi_0(\beta - \rho x_0) + 1, \quad (32)$$

$$\text{sign}\left(\frac{d\phi}{dt}\right) = \text{sign}(\psi_0), \quad \psi_0 \neq 0. \quad (33)$$

Note that by (33) $\phi(t)$ is obviously a strictly monotonous function. In such a way, $\phi(t)$ either vanishes at a single isolated point only, or it never vanishes. As $\psi_0 \neq 0$, only the following four options are possible for $u^*(t)$ to be optimal.

- (1) If $\psi_0 > (\rho x_0 - \beta)^{-1} > 0$, then $\phi(0) > 0$ and $\frac{d\phi(t)}{dt} > 0, \forall t \geq 0$, which means $\phi(t) > 0, \forall t \geq 0$. By (29), then $u^*(t) \equiv 0$. However, it is clear from (26) that (17) with $u(t) \equiv u^*(t) \equiv 0$ does not satisfy (20).
- (2) If $(\rho x_0 - \beta)^{-1} > \psi_0 > 0$, then $\phi(0) < 0$ and $\frac{d\phi(t)}{dt} > 0, \forall t \geq 0$. By (29), then $u^*(t) = \bar{u}, t < t_{sw}$ and $u^*(t) = 0, t > t_{sw}$. However, this option is not possible because $(\rho x_0 - \beta) > 0$ contradicts the assumption (21) as α, \bar{u} and x_0 are positive.
- (3) If $\psi_0 < (\rho x_0 - \beta)^{-1} < 0$, then $\phi(0) < 0$ and $\frac{d\phi(t)}{dt} < 0, \forall t \geq 0$, which means $\phi(t) < 0, \forall t \geq 0$. By (29), then $u^*(t) \equiv \bar{u}$. However, by assumption (21) and by (26) it holds that $x(t_f) > x_0$. Thus, (20) is violated.
- (4) If $(\rho x_0 - \beta)^{-1} < \psi_0 < 0$, then $\phi(0) > 0$ and $\frac{d\phi(t)}{dt} < 0, \forall t \geq 0$. By (29), then

$$u^*(t) = 0, t < t_{sw}, u^*(t) = \bar{u}, t > t_{sw}; \quad t_{sw} = \alpha^{-1} \log((\rho x_0 \psi_0 - 1)/(\beta \psi_0)). \quad (34)$$

Moreover, it can be seen through some straightforward analysis that when ψ_0 ranges through $((\rho x_0 - \beta)^{-1}, 0)$, the expression $((\rho x_0 \psi_0 - 1)/(\beta \psi_0))$ ranges through $(1, \infty)$, i.e. ψ_0 can always be chosen in such a way that any $t_{sw} \in (0, \infty)$ is possible.

Summarising, the control satisfying PMP and (20) under assumption (21) should have the form (34) for some suitable switching time t_{sw} . To conclude the proof, it remains to show that there is a unique $t_{sw} \in [0, t_f]$ such that (17) with $u(t) \equiv u^*(t)$ given by (34) satisfies the boundary conditions (20). Such a property follows straightforwardly by (26) and (21), moreover, also by (26), the switching time t_{sw} is the solution of

$$x_0 = \exp((- \alpha - \rho \bar{u})(t_f - t_{sw})) \left(\exp(-\alpha t_{sw}) x_0 - \frac{\beta \bar{u}}{\alpha + \rho \bar{u}} \right) + \frac{\beta \bar{u}}{\alpha + \rho \bar{u}}. \quad (35)$$

Note, that t_{sw} solving (35) is unique for any given $t_f > 0$. Indeed, the right-hand side of (35) is a smooth function of t_{sw} and it is equal to $\exp(-\alpha t_f) x_0 < x_0$ if $t_{sw} = t_f$ and to

$$\exp((- \alpha - \rho \bar{u}) t_f) \left(x_0 - \frac{\beta \bar{u}}{\alpha + \rho \bar{u}} \right) + \frac{\beta \bar{u}}{\alpha + \rho \bar{u}} > x_0,$$

if $t_{sw} = 0$. The last inequality straightforwardly holds thanks to the assumption (21) and $\exp((- \alpha - \rho \bar{u}) t_f) \in (0, 1)$. As a consequence, there exists at least one t_{sw} solving (35) thanks to the well-known basic property of continuous functions. To show that such t_{sw} is unique, note that by (35) and the implicit function theorem, there exists locally defined smooth function $t_{sw}(t_f)$ and

$$\frac{dt_{sw}}{dt_f} = 1 + \frac{\alpha x_0}{(\rho x_0 - \beta \exp(\alpha t_{sw})) \bar{u}}, \quad (36)$$

i.e. by (21) it holds that $(dt_{sw})/(dt_f) > 0$ and $t_{sw}(t_f)$ is monotonously growing and therefore globally defined and one to one. As a consequence, t_{sw} is unique and the proof is complete. \square

Remark 4. The assumption (21) is equivalent to $\alpha x_0/(\beta - \rho x_0) \in (0, \bar{u})$. The value $\alpha x_0/(\beta - \rho x_0)$ is the constant trim control keeping the state x_0 as the equilibrium, i.e. $x(t) \equiv x_0$ and therefore the assumption (21) should be valid in any reasonable practical setting. Indeed, if the assumption (21) is to be replaced by $(\beta - \rho x_0)\bar{u} - \alpha x_0 = 0$, then the optimal control is $u^*(t) = \bar{u}$, $\forall t \in [0, t_f]$, i.e. as if $t_{sw} = 0$ in (34). As such, $\bar{u} = \alpha x_0/(\beta - \rho x_0)$ is the trim control value that ensures $x(t) \equiv x_0$; practically, such a situation is not acceptable because any small perturbation pushing the state to a value slightly lower than x_0 cannot be compensated for.

Remark 5. We consider the optimal control law with the state constraint (20) because a single operating temperature x_0 for the scheduling problem is considered. Definitely, the furnace temperature is x_0 at the beginning of each idle period and should also be x_0 at the end of the idle period to execute the consecutive task. In fact, Theorem 5.1 can be easily extended to a more general case with boundary conditions of the form $x(0) = x_0$, $x(t_f) = x_f$, $x_0 > 0$, $x_f > 0$ and, possibly, $x_0 \neq x_f$.

Let us finally show that the energy function of the idle period length, for a furnace described by the bilinear model (17) and optimally controlled as proposed in Theorem 5.1, is concave.

Theorem 5.2. *The idle energy function of system (17) under control (22) assuming (21) is described as $E(t_f) = \bar{u}(t_f - t_{sw}(t_f))$, and it is concave.*

Proof. Recall from the proof of Theorem 5.1 that t_{sw} in control (22) applied to system (17) is uniquely determined with the implicit solution of (35) for given parameters α , β , ρ , x_0 , and \bar{u} . Thus, the energy consumption during an idle period, i.e. idle energy function, can be described as

$$E(t_f) = \bar{u}(t_f - t_{sw}(t_f)). \quad (37)$$

Then, for concavity of $E(t_f)$, it remains to show that

$$\frac{\partial^2 E(t_f)}{\partial t_f^2} = -\bar{u} \frac{d^2 t_{sw}}{dt_f^2} \quad (38)$$

is negative $\forall t_{sw}$. Substituting further differentiation of (36) to (38) gives

$$\frac{\partial^2 E(t_f)}{\partial t_f^2} = -\frac{\alpha^2 \beta x_0 \exp(\alpha t_{sw})}{(\rho x_0 - \beta \exp(\alpha t_{sw}))^2} \frac{dt_{sw}}{dt_f} < 0 \quad \forall t_{sw}, \quad (39)$$

because $\beta > 0$, $x_0 > 0$ and $(dt_{sw})/(dt_f) > 0$ as already shown in the proof of Theorem 5.1. As a consequence, $E(t_f)$ is concave and the proof is complete. \square

By Theorem 5.2, we conclude that the energy-optimal scheduling algorithm proposed in Section 3.3 can be performed in polynomial time for furnaces that can be modelled as (17), and controlled by (22).

5.3. Case Study: An industrial electric furnace

Škoda Auto has a production line employing a ModulTherm[®] system by ALD, containing electric vacuum furnaces used for the steel hardening. Each furnace contains

three heating elements, distributed around the circumference of the furnace. The outer steel shells of the furnaces are cooled by a central cooling system of circulating water at $\sim 35^\circ\text{C}$ to avoid overheating of the system. Thus, we can assume that the ambient temperature (T_e) is constant. The operating temperature of the furnaces is set to 960°C for the hardening process. The average time needed for material heating is about 2.5 hours.

The heating of the furnaces has a substantial energy demand across the whole production line. In a normal regime, all furnaces are turned on and heated to the operating temperature. The operating temperature is preserved even if nothing is being processed. To investigate the potential for energy savings, an experiment has been performed, during which the furnace cooled to 600°C , and its steady-state power consumption was measured. Afterwards, the furnace was heated back to the operating temperature again. Measured data are shown in Figure 3 (Dušek 2016). The steady-state power consumption for 600°C and for 960°C are about 18 kW and 39 kW, respectively.

Clearly, if the idle period is long enough, significant energy savings can be achieved by lowering the temperature of the furnace, i.e. turning off the furnace for a longer time. However, the slow dynamics, i.e. the time needed for cooling and reheating of a furnace, should be considered with respect to the parameters of the tasks in the scheduling problem, to reach the operating temperature for any task at the desired time. To address this issue, we propose an approximate energy-optimal solution by utilising the bilinear model (17) and the optimal control law by Theorem 5.1 based on that approximate model. In the following, we apply the utilised model and the proposed optimal control.

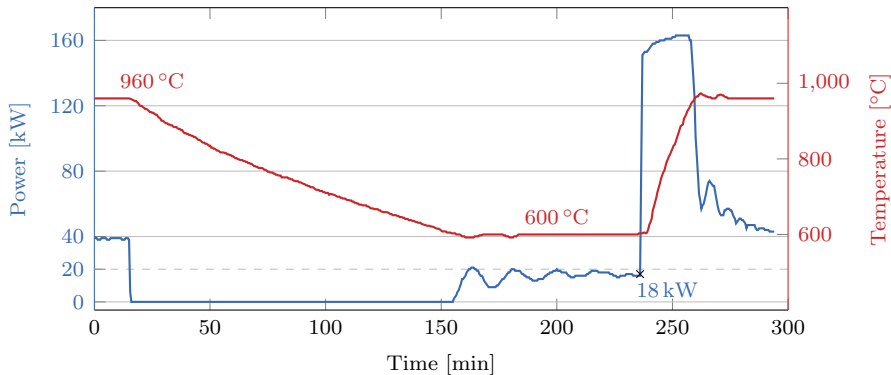


Figure 3. Relationship between temperature and power when cooling to 600°C and heating back to operating temperature

5.3.1. Parameter estimation of the bilinear model

We employ the bilinear model given by (17) to the furnace mentioned above and estimate the parameters α , β , ρ in the model. For this purpose, we use the temperature data collected by Dušek (2016) shown by dashed lines in Figure 4, with a sampling time of 30 s. The system parameters are estimated as

$$\alpha = 0.003821964, \quad \beta = 0.175187494, \quad \rho = 0.00008666 \quad (40)$$

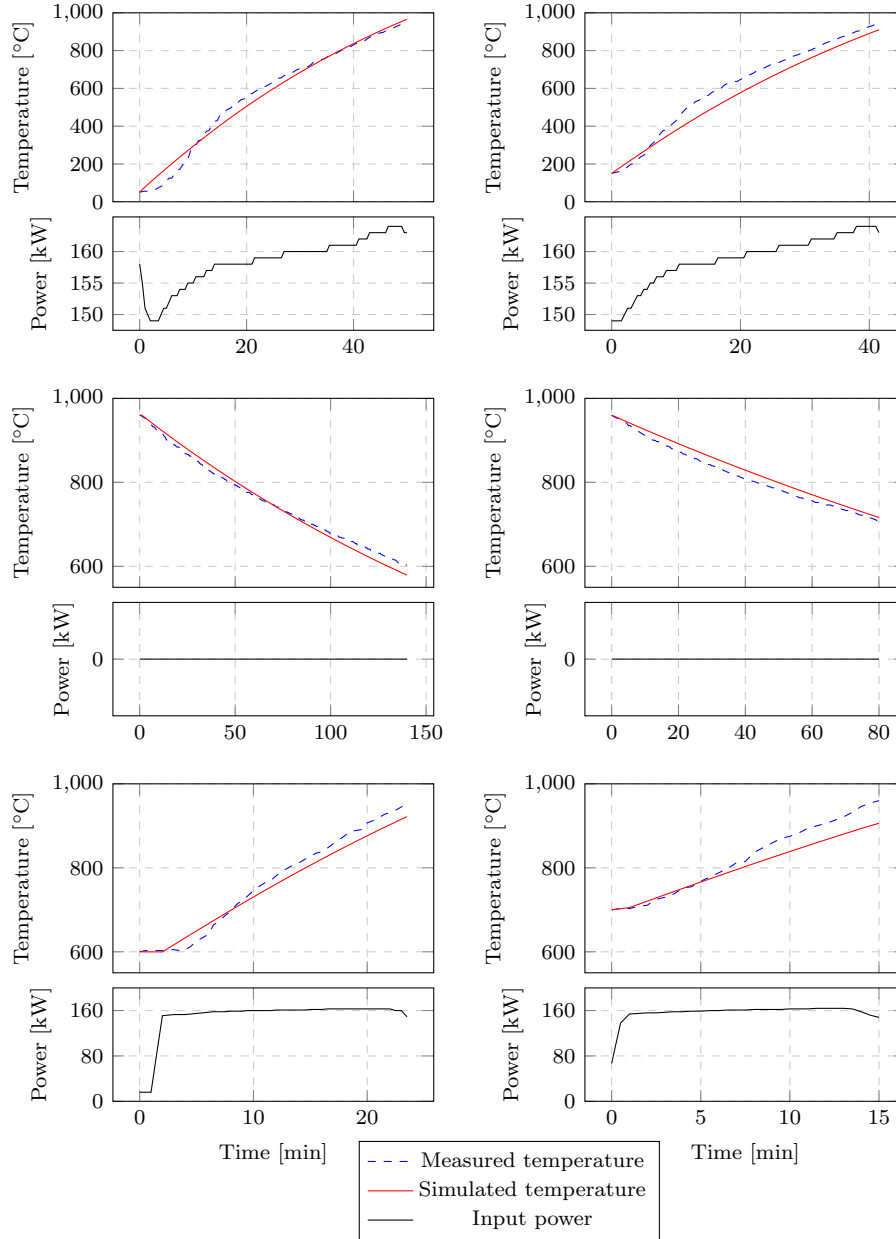


Figure 4. Comparison of the measured data and simulation using a bilinear model.

by the least-squares method using the measured temperature samples and their derivatives obtained via a polynomial regression. The simulated response of the system (17) with (40) is illustrated by solid lines in Figure 4, when the experimental input power is applied. The mean absolute percentage error over all experiments for the identified model is found as 4.21 %, which is acceptable for system identification.

Remark 6. Note that the restricted range of the input signal was applied due to the availability of the furnace in production, see Dušek (2016). Indeed, more various types of input power could be applied for better identification. Nevertheless, we think that the collected data are sufficient for identification, in the sense of applied step input in

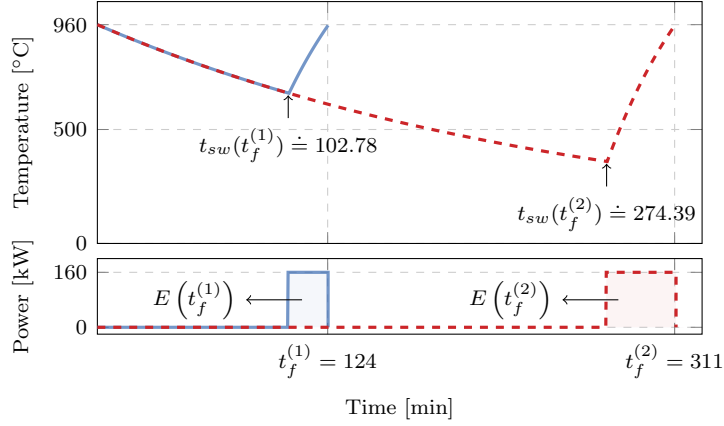


Figure 5. Example of the optimal control for two different terminal times $t_f^{(1)}$ and $t_f^{(2)}$.

open-loop optimal control.

5.3.2. Optimal control of the furnace and the related idle energy function

In Figure 5, the time response of system (17) with the parameters (40) is illustrated via simulations for two different terminal times, i.e. idle periods, when the optimal control (22) is applied. Here, we should note for the real furnace that the proposed control may not be precisely optimal, and the operating temperature may not be reached exactly at $t = t_f$, inherently due to uncertain dynamics and approximate modelling. Nevertheless, the proposed approximation is acceptable for achieving almost optimal control in practice, and the reach of operating temperature can be guaranteed with a simple *if case* control as is actually done in switching to feedback control around the operating point in practical process control approaches.

Let us now illustrate the idle energy function (37) for the system (17) with (40) under control (22), via an appropriate sampling of t_f , and finding t_{sw} implicitly from (23). The resulting idle energy function denoted by E_{cont} is depicted in Figure 6, where t_f denotes the idle period length. Function E_{cont} is bounded by a constant shown by the dashed line, which is the energy for heating the machine from the ambient temperature (35 °C) to the processing temperature (960 °C). Clearly, it is seen that E_{cont} is concave, as declared by Theorem 5.2.

As mentioned previously, common scheduling approaches to idle energy optimisation assume only a small number of machine modes with constant transition times (costs) between them, see Mouzon, Yildirim, and Twomey (2007); Shrouf et al. (2014); Che, Zhang, and Wu (2017). Therefore, we also model two simple cases with a single standby mode for the comparison of scheduling approaches in the following section. In these two cases, the furnace is either heated to 960 °C (processing temperature) or switched to a standby mode, for which the temperature is lower. If the idle period is long enough, the machine cools to the respective standby temperature, then the temperature is maintained as long as possible, and the furnace is heated back such that it reaches 960 °C at the end of the idle period. The standby temperatures are fixed to 700 °C and 600 °C, respectively. The corresponding idle energy functions E_{700} and E_{600} are shown in Figure 6. The slope of their first segment is equal to the energy compensating the losses when the furnace is heated to the processing temperature (960 °C), whereas the slope of the second segment corresponds to the energy needed to compensate for

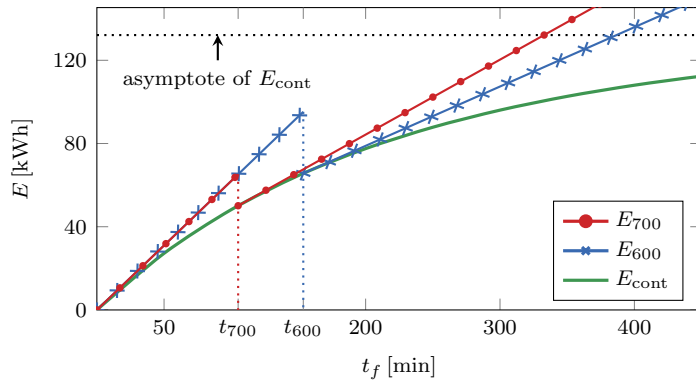


Figure 6. Idle energy function E_{cont} corresponding to the approach proposed in this work and its variants E_{600} and E_{700} corresponding to the common approach modelling only a single non-processing mode.

the losses for maintaining the standby temperature. The discontinuities at times t_{700} and t_{600} indicate the time when the idle period length is equal to the time needed for the transition (cooling to the standby temperature and re-heating to the processing temperature again).

Note that E_{cont} gives a lower bound to E_{700} and E_{600} , as these two model only a subset of all possible standby temperatures captured by E_{cont} .

6. Numerical experiments

We perform scheduling experiments for the case study given above. The furnace model (17) with parameters (40) is used. To show the potential of the proposed approach, we compare energy consumption savings achieved for different energy functions in Section 6.2. In addition, we investigate the performance of the ILP model with respect to the number of linear segments used for the approximation of the idle energy function and compare the results to the graph-based approach in Section 6.3. All experiments were performed on a Dell PC with an Intel Core i7-4610M CPU operating at 3 GHz, 16 GB RAM.

6.1. Benchmark instances

For the experiments, a set of 6750 instances was generated using Algorithm 1. Specifically, 10 instances were generated for each combination of $n \in \{30, 40, 50\}$, $\gamma \in \{0.2, 0.4, \dots, 3.0\}$, and $\delta \in \{0.2, 0.4, \dots, 3.0\}$. A wide range of parameters γ and δ was used to generate data of different characteristics. Constants p_{\min} and p_{\max} , denoting the minimal and the maximal processing time, were set to 1 and 300, respectively. By $U\{a, b\}$, we denote integer uniform distribution on set $\{a, a+1, \dots, b\}$; here $Exp(x)$ denotes exponential distribution with scale parameter x .

One of the factors influencing the final energy savings is the utilisation of the machine, which is calculated as the ratio between the sum of processing times and length of the scheduling horizon, i.e. $\sum_{i=1}^n p_i / (\tilde{d}_n - r_1)$. Based on the machine utilisation, the generated instances were divided, as indicated by Table 2.

Algorithm 1: Generation of task parameters

input : Number of tasks n , bounds on processing time p_{\min}, p_{\max} , parameters γ, δ
output: Vectors $\mathbf{r}, \tilde{\mathbf{d}}, \mathbf{p}$

```
// generate processing times
foreach  $i \leftarrow 1$  to  $n$  do  $p_i \sim U\{p_{\min}, p_{\max}\}$ ;

// generate release times and deadlines
 $r_1 := 0$ ;
 $\tilde{d}_1 \sim \lceil r_1 + p_1 + \text{Exp}(\delta \cdot \text{Average}(\mathbf{p})) \rceil$ ;
foreach  $i \leftarrow 2$  to  $n$  do
     $r_i \sim \lceil r_{i-1} + p_{i-1} + \text{Exp}(\gamma \cdot \text{Average}(\mathbf{p})) \rceil$ ;
     $\tilde{d}_i \sim \lceil r_i + p_i + \text{Exp}(\delta \cdot \text{Average}(\mathbf{p})) \rceil$ ;

// propagate deadlines by (3) (release times are already propagated)
foreach  $i \leftarrow (n-1)$  to  $1$  do  $\tilde{d}_i := \min\{\tilde{d}_{i+1} - p_{i+1}, \tilde{d}_i\}$ ;
```

Table 2. Number of generated instances with respect to utilisation (columns) and number of tasks (rows).

		Utilisation							
		(0.1, 0.2]	(0.2, 0.3]	(0.3, 0.4]	(0.4, 0.5]	(0.5, 0.6]	(0.6, 0.7]	(0.7, 0.8]	(0.8, 0.9]
n	30	24	1060	1244	778	574	390	250	180
	40	4	1010	1346	768	548	378	226	220
	50	10	1036	1346	748	502	398	236	224
Total		38	3106	3936	2294	1624	1166	712	624

6.2. Energy consumption under different idle energy functions

For the experiment, we optimised all generated instances with respect to the idle energy functions E_{cont} , E_{600} , and E_{700} depicted in Figure 6. In addition, we assumed a system with two standby modes with the temperatures fixed to 600 °C and 700 °C, and the corresponding idle energy function defined as $E_{600,700}(t_f) = \min\{E_{600}(t_f), E_{700}(t_f)\}$.

Instances with function E_{cont} were optimised by the energy graph approach (see Section 3.3). However, functions E_{600} , E_{700} , and $E_{600,700}$ are not concave, and so the ILP model (14)-(16) was used for the optimisation instead. The ILP model was optimised by the state-of-the-art solver Gurobi (v8.1). Default parameters of the solver were used.

The average (maximum) solving time was 0.05 s (0.25 s) for the energy graph approach and 0.09 s (7.77 s) for the ILP. Results showed that the ILP needed about two times more time on average when optimising instances with $E_{600,700}$ (which has three linear segments), compared to instances with both E_{600} and E_{700} (which have only two linear segments). This indicates that the performance of the ILP solver depends on the number of segments approximating the energy function. A further experiment is described in Section 6.3.

To compare different idle energy functions, we define the average power per idle time \bar{P} as

$$\bar{P} = \frac{E_{\text{total}}^*}{(\tilde{d}_n - r_1) - \sum_{i=1}^n p_i}, \quad (41)$$

where E_{total}^* is the optimal total idle energy consumption (with respect to given idle energy function). It is assumed that the machine is underutilised, i.e. $(\tilde{d}_n - r_1) - \sum_{i=1}^n p_i > 0$. For the considered idle energy functions, it holds that $0 \leq \bar{P} \leq \bar{P}_{\text{max}}$, where \bar{P}_{max} is the theoretical worst case, representing the situation when the furnace is heated to the operating temperature all the time.

Results for different utilisation of the machines are shown in the form of boxplots in Figure 7. Clearly, our approach using E_{cont} dominates all other idle energy functions, as the power saving modes modelled by E_{600} , E_{700} , and $E_{600,700}$ are only a subset of all possible modes considered by E_{cont} . The difference increases when utilisation is lowered as the idle periods become longer. For example, the average \bar{P} for E_{cont} is less than half compared to $E_{600,700}$ for utilisation $(0.1, 0.2]$.

It can be seen that \bar{P} optimised with respect to E_{600} nearly converges to steady-state power compensating for the energy loss at 600 °C, which is approximately 18 kW. Similar observation also holds for E_{700} , and $E_{600,700}$.

Using E_{700} is slightly better than E_{600} only when the utilisation is high because shorter idle periods do not allow the standby mode corresponding to 600 °C to be reached. This can be intuitively seen in Figure 6 as $E_{700} < E_{600}$ only on interval $[t_{700}, t_{600})$.

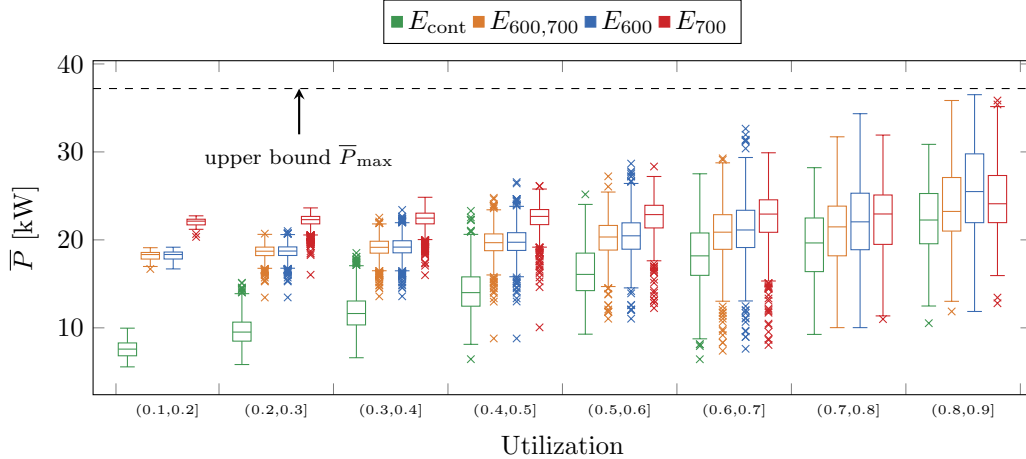


Figure 7. Relationship of the idle energy function E and \bar{P} depending on utilisation of the machine.

6.3. Performance of the ILP model with respect to the number of idle energy function segments

In this experiment, we measured the performance of the ILP model with respect to the number of linear segments, denoted by $\#segments$, approximating E_{cont} . Specifically, we measured the average solving time and the average optimality gap for $\#segments \in \{2, 3, \dots, 12\}$. To get the optimality gap, the instances were scheduled w.r.t. the approximated idle energy function but evaluated w.r.t. E_{cont} representing the optimal control. To find the breakpoints on the interval $[0 \text{ min}, 5000 \text{ min}]$, the Python library *pwlif* was used (Jekel and Venter 2019). Illustration for two and four approximating line segments is shown in Figure 8.

Results of the experiments are shown in Figure 9. There, the plotted points represent the average values (across all 6750 instances), and the filled area represents

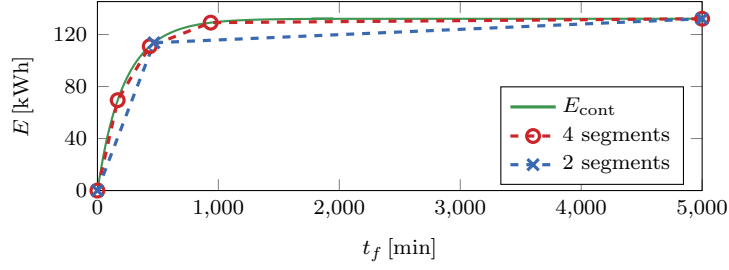


Figure 8. Approximation of E_{cont} by 2 and 4 linear segments.

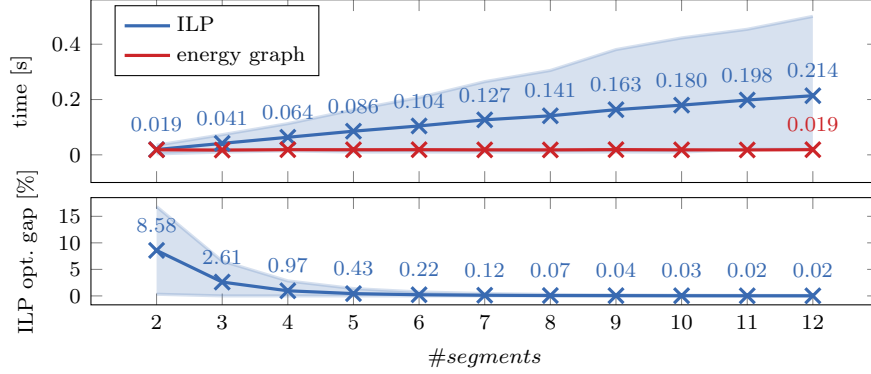


Figure 9. Performance of the ILP model for different $\#segments$, and the corresponding optimality gap for schedules found w.r.t. the approximated energy function but evaluated by E_{cont} .

the standard deviation bounded from the top (bottom) by the maximum (minimum) observed value.

Note that the piecewise linear functions approximating E_{cont} are concave. Therefore, the graph-based approach can be used as well. Both approaches lead to the same optimal objective when optimising w.r.t. the same idle energy function. However, the graph-based approach needs only a finite number of the values to label the edges of the energy graph, while the ILP model needs to represent the whole idle energy function explicitly (using its piecewise linear approximation). The average runtimes of the graph-based approach are shown in Figure 9 for comparison. Clearly, the time needed to solve the ILP model increases with the increasing $\#segments$ whereas the time needed by the graph-based approach remains constant.

7. Conclusions

This article provides a novel approach to idle energy consumption minimisation of the industrial furnaces. Both optimal scheduling and optimal control of continuous-time dynamical systems have been considered to achieve the greatest possible energy savings. The complex dynamics of the furnace is modelled by a continuous-time bilinear system model, which has been analysed using Pontryagin’s minimum principle. Based on the resulting optimal control law, the idle energy function has been derived, and its concavity has been proven. By using this crucial property, it has been shown that the addressed scheduling problem can be solved in polynomial time by the proposed efficient graph-based algorithm. In the case study, parameters of the bilinear model have been estimated using the real data measured at Škoda Auto. The results of the

numerical study show that our approach addressing both scheduling and control dominates the existing approaches, which consider only a small set of energy-saving modes. Also, the proposed graph-based algorithm exhibits better performance, compared with the ILP model.

Disclosure statement

No potential conflict of interest was reported by the authors.

Acknowledgement

The authors want to thank Josef Dušek from Škoda Auto for carrying out the analysis of the hardening line. Furthermore, we are glad to acknowledge the help of Jan Skočilas from the Faculty of Mechanical Engineering, Czech Technical University in Prague, who provided insights into the field of electric furnaces. Last but not least, we thank our colleague Matěj Novotný, for his ideas that helped us analyse the idle energy function.

This work was funded by Ministry of Education, Youth and Sport of the Czech Republic within the project Cluster 4.0 number CZ.02.1.01/0.0/0.0/16_026/0008432; and European Regional Development Fund under the project Robotics for Industry 4.0 (reg. no. CZ.02.1.01/0.0/0.0/15_0030000470).

References

- Aghelinejad, M., Y. Ouazene, and A. Yalaoui. 2018. “Production scheduling optimisation with machine state and time-dependent energy costs.” *International Journal of Production Research* 56 (16): 5558–5575.
- Angel, E., E. Bampis, and V. Chau. 2012. “Low Complexity Scheduling Algorithm Minimizing the Energy for Tasks with Agreeable Deadlines.” In *LATIN 2012: Theoretical Informatics*, edited by D. Fernández-Baca, Berlin, Heidelberg, 13–24. Springer Berlin Heidelberg.
- Baker, K.R., and D. Trietsch. 2009. *Principles of Sequencing and Scheduling*. Wiley Publishing.
- Baptiste, P., M. Chrobak, and C. Dürr. 2012. “Polynomial-time Algorithms for Minimum Energy Scheduling.” *ACM Trans. Algorithms* 8 (3): 136–150.
- Che, A., X. Wu, J. Peng, and P. Yan. 2017. “Energy-efficient bi-objective single-machine scheduling with power-down mechanism.” *Computers & Operations Research* 85: 172–183.
- Che, A., S. Zhang, and X. Wu. 2017. “Energy-conscious unrelated parallel machine scheduling under time-of-use electricity tariffs.” *Journal of Cleaner Production* 156: 688 – 697.
- Chee Chook, K., and A.H. Tan. 2007. “Identification of an Electric Resistance Furnace.” *IEEE Transactions on Instrumentation and Measurement* 56: 2262 – 2270.
- Cormen, T.H., C.E. Leiserson, R.L. Rivest, and C. Stein. 2001. *Introduction to Algorithms*. 2nd ed. Cambridge, MA, USA: MIT Press.
- Derese, I., and E.J. Nodulus. 1980. “Nonlinear control of bilinear systems.” *IEE Proceedings D: Control Theory and Applications* 127 (4): 169–175.
- Dušek, J. 2016. “Návrh úpravy řízení výrobní linky s ohledem na snížení její spotřeby.” Master’s thesis, Czech Technical University in Prague, the Czech republic. <https://dspace.cvut.cz/handle/10467/65284>.
- Gahm, C., F. Denz, M. Dirr, and A. Tuma. 2016. “Energy-efficient scheduling in manufacturing companies: A review and research framework.” *European Journal of Operational Research* 248 (3): 744 – 757.

- Garey, M., and D. Johnson. 1977. “Two-Processor Scheduling with Start-Times and Deadlines.” *SIAM Journal on Computing* 6 (3): 416–426.
- Gerards, M.E.T., and J. Kuper. 2013. “Optimal DPM and DVFS for Frame-based Real-time Systems.” *ACM Trans. Archit. Code Optim.* 9 (4): 41:1–41:23.
- Gutowski, T., C. Murphy, D. Allen, D. Bauer, B. Bras, T. Piwonka, P. Sheng, J. Sutherland, D. Thurston, and E. Wolff. 2005. “Environmentally benign manufacturing: Observations from Japan, Europe and the United States.” *Journal of Cleaner Production* 13: 1–17.
- Haït, A., and C. Artigues. 2011. “A hybrid CP/MILP method for scheduling with energy costs.” *European Journal of Industrial Engineering* 5: 471–489.
- Irani, S., S. Shukla, and R. Gupta. 2003. “Online Strategies for Dynamic Power Management in Systems with Multiple Power-saving States.” *ACM Trans. Embed. Comput. Syst.* 2 (3): 325–346.
- Jekel, C.F., and G. Venter. 2019. *pwlfit: A Python Library for Fitting 1D Continuous Piecewise Linear Functions*. Accessed 2019-08-16. https://github.com/cjekel/piecewise_linear_fit_py.
- Kirk, D.E. 2004. *Optimal Control Theory: An Introduction*. Dover Books on Electrical Engineering Series. Dover Publications.
- Liu, C.-H., and D.-H. Huang. 2014. “Reduction of power consumption and carbon footprints by applying multi-objective optimisation via genetic algorithms.” *International Journal of Production Research* 52 (2): 337–352.
- Liu, M., X. Yang, F. Chu, J. Zhang, and C. Chu. 2018. “Energy-oriented bi-objective optimization for the tempered glass scheduling.” *Omega (United Kingdom)* 101995.
- Módos, I., P. Šúcha, and Z. Hanzálek. 2017. “Algorithms for robust production scheduling with energy consumption limits.” *Computers & Industrial Engineering* 112: 391 – 408.
- Moon, U.-C., and K.Y. Lee. 2003. “Hybrid algorithm with fuzzy system and conventional PI control for the temperature control of TV glass furnace.” *IEEE Transactions on Control Systems Technology* 11 (4): 548 – 554.
- Mouzon, G., M. Yildirim, and J. Twomey. 2007. “Operational methods for minimization of energy consumption of manufacturing equipment.” *International Journal of Production Research* 45: 4247–4271.
- Shrouf, F., J. Ordieres, Á. García-Sánchez, and M. Ortega-Mier. 2014. “Optimizing the production scheduling of a single machine to minimize total energy consumption costs.” *Journal of Cleaner Production* 67: 197–207.
- Tang, L., H. Ren, and Y. Yang. 2014. “Reheat furnace scheduling with energy consideration.” *International Journal of Production Research* 53: 1–19.
- Wang, J., and C.J. Spanos. 2002. “Real-time furnace modeling and diagnostics.” *IEEE Transactions on Semiconductor Manufacturing* 15 (4): 393–403.
- Wang, Q.-G., C.-C. Hang, and W. Zou. 1998. “Automatic tuning of nonlinear PID controllers for unsymmetrical processes.” *Computers & Chemical Engineering* 22 (4-5): 687–694.
- Yu, D.-L. 2000. “Diagnosing simulated faults for an industrial furnace based on bilinear model.” *IEEE Transactions on Control Systems Technology* 8 (3): 435–442.
- Zhang, B., Z. Chen, L. Xu, J. Wang, J. Zhang, and H. Shao. 2002. “The modeling and control of a reheating furnace.” In *Proceedings of the 2002 American Control Conference*, Vol. 5, May, 3823–3828 vol.5.